Molecular Biology of the Cell
Vol. 19, 5435–5445, December 2008

Role of LPA_4/p2y9/GPR23 in Negative Regulation of Cell Motility

Zendra Lee,* Ching-Ting Cheng,* Helen Zhang,† Mark A. Subler,† Jinhua Wu,* Abir Mukherjee,* Jolene J. Windle,† Ching-Kang Chen,* and Xianjun Fang*

Departments of *Biochemistry and Molecular Biology and †Human Genetics, and Massey Cancer Center, Virginia Commonwealth University School of Medicine, Richmond, VA 23298

Submitted March 26, 2008; Revised August 20, 2008; Accepted September 25, 2008
Monitoring Editor: Carl-Henrik Heldin

Lysophosphatidic acid (LPA) is a ligand of multiple G protein–coupled receptors. The $LPA_{1–3}$ receptors are members of the endothelial cell differentiation gene (Edg) family. LPA_4/p2y9/GPR23, a member of the purinergic receptor family, and recently identified LPA_5/GPR92 and p2y5 are structurally distant from the canonical Edg LPA receptors. Here we report targeted disruption of *lpa_4* in mice. Although LPA_4-deficient mice displayed no apparent abnormalities, LPA_4-deficient mouse embryonic fibroblasts (MEFs) were hypersensitive to LPA-induced cell migration. Consistent with negative modulation of the phosphatidylinositol 3 kinase pathway by LPA_4, LPA_4 deficiency potentiated Akt and Rac but decreased Rho activation induced by LPA. Reconstitution of LPA_4 converted LPA_4-negative cells into a less motile phenotype. In support of the biological relevance of these observations, ectopic expression of LPA_4 strongly inhibited migration and invasion of human cancer cells. When coexpressed with LPA_1 in B103 neuroblastoma cells devoid of endogenous LPA receptors, LPA_4 attenuated LPA_1-driven migration and invasion, indicating functional antagonism between the two subtypes of LPA receptors. These results provide genetic and biochemical evidence that LPA_4 is a suppressor of LPA-dependent cell migration and invasion in contrast to the motility-stimulating Edg LPA receptors.

INTRODUCTION

Lysophosphatidic acid (LPA, 1-acyl-*sn*-glycerol-3-phosphate) is produced by activated platelets during coagulation and thus is a normal constituent of serum (Eichholtz *et al.*, 1993; Sano *et al.*, 2002). At least six G protein–coupled receptors (GPCRs) have been identified to mediate a wide range of biological functions of LPA (Hecht *et al.*, 1996; An *et al.*, 1998; Bandoh *et al.*, 1999; Im *et al.*, 2000; Noguchi *et al.*, 2003; Lee *et al.*, 2006; Pasternack *et al.*, 2008). The LPA_1/Edg2, LPA_2/Edg4 and LPA_3/Edg7 receptors are members of the endothelial cell differentiation gene (Edg) family, sharing 50–57% homology in their amino acid sequences (Hecht *et al.*, 1996; An *et al.*, 1998; Bandoh *et al.*, 1999; Im *et al.*, 2000). LPA_4/GPR23/p2y9, a member of the purinergic receptor family, and the related LPA_5/GPR92 and p2y5 were structurally distant from the Edg $LPA_{1–3}$ receptors (Noguchi *et al.*, 2003; Lee *et al.*, 2006; Pasternack *et al.*, 2008). LPA receptors couple to multiple G proteins, G12/13, Gi, Gq, and probably Gs that in turn, activate diverse pathways including stimulation of phospholipase C and D, small GTPases, mitogen-activated protein kinases, and phosphatidylinositol 3-kinase (PI3K; van der Bend *et al.*, 1992; Howe and Marshall,1993; An *et al.*, 1998; Bandoh *et al.*, 1999; Im *et al.*, 2000; Mills and Moolenaar, 2003; van Meeteren and Moolenaar, 2007). Activation of these signaling events downstream of LPA receptors culminates in cytoskeleton remodeling, cell proliferation, survival and migration (Mills and Moolenaar, 2003; van Meeteren and Moolenaar, 2007). In addition to these cell surface GPCRs, LPA has been shown to bind and activate the peroxisome proliferator-activated receptor γ (PPARγ) which plays critical roles in controlling fat and energy metabolism (McIntyre *et al.*, 2003).

Only minor phenotypic changes were seen in LPA_1 or LPA_2 receptor-deficient mice (Contos *et al.*, 2000, 2002). When the *lpa_1* knockout mice were studied under pathophysiological conditions, however, essential roles for LPA_1 in the initiation of neuropathic pain and promotion of pulmonary and renal fibrosis were unraveled (Inoue *et al.*, 2004; Pradere *et al.*, 2007; Tager *et al.*, 2008). Homozygous deletion of the LPA_3 receptor leads to a delayed implantation and defective embryo spacing, associated with reduced uterine expression of Cox-2 mRNA (Ye *et al.*, 2005). Although these roles for individual receptors have been identified, more profound effects such as early embryonic lethality have not been observed from single or even double receptor knockouts (Contos *et al.*, 2000, 2002; Ye *et al.*, 2005). These results are in contrast to deletion studies of the LPA-synthesizing enzyme autotoxin (ATX) where homozygous deletion results in embryonic lethality at embryonic day (E)9.5 due to impaired vessel formation in the yolk sac and embryo proper (Tanaka *et al.*, 2006; van Meeteren, 2006). These results suggest involvement of LPA_4, LPA_5, or other unidentified receptors as effectors of ATX. In the current study, we disrupted the LPA_4-encoding gene (*lpa_4/p2Y9/gpr23*) in mice. Similar to deletion of *lpa_1* or *lpa_2* (Contos *et al.*, 2000, 2002), LPA_4-deficient mice did not show obvious abnormalities in embryonic development, fertility or normal physiology. However, analysis of LPA_4-negative cells from *lpa_4* knockout (KO) mice revealed a novel role for LPA_4 in the negative

This article was published online ahead of print in *MBC in Press* (http://www.molbiolcell.org/cgi/doi/10.1091/mbc.E08–03–0316) on October 8, 2008.

Address correspondence to: Xianjun Fang (xfang@vcu.edu).

Abbreviations used: LPA, lysophosphatidic acid; GPCR, G protein–coupled receptor; KO, knockout; MEF, mouse embryonic fibroblast.

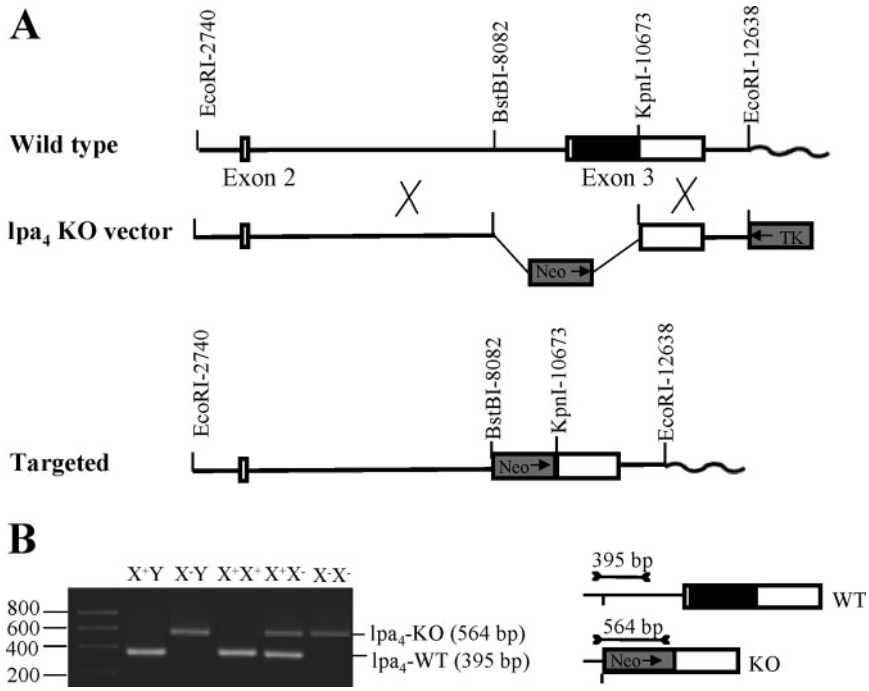

Figure 1. Generation of LPA_4-deficient mice. (A) The targeting vector pKO Scrambler NTKV-1901 containing the *neo* gene was used to replace the 3′ portion of intron 2 and the 5′ fragment of exon 3 of the *lpa*$_4$ gene. The 5′ fragment of exon 3 carries the entire coding sequence of LPA_4. (B) PCR analysis of genomic DNA confirms the DNA arrangements consistent with X^+Y, X^-Y, X^+X^+, X^+X^-, and X^-X^- genotypes. The relative locations of three primers used for PCR detection of WT and KO alleles are indicated.

control of cell migration. Stimulation of cell motility is one of the major biological effects of LPA and its producing enzyme ATX (Umezu-Goto *et al.*, 2002; Mills and Moolenaar, 2003; van Meeteren and Moolenaar, 2007). LPA-induced cell migration is mediated mainly by LPA_1 although LPA_2 or LPA_3 may be also capable of evoking the response in various cellular contexts (Shida *et al.*, 2003; Hama *et al.*, 2004;Chan *et al.*, 2007; Chen *et al.*, 2007). However, little is known about how the migratory response to LPA is appropriately controlled in mammalian cells that usually coexpress multiple LPA receptor subtypes. The results of the present study using LPA_4-deficient cells and other cellular models identify LPA_4 as a suppressor of LPA-mediated cell migration and invasion.

MATERIALS AND METHODS

Reagents

1-Oleoly (18:1) LPA was obtained from Avanti Polar Lipids (Alabaster, AL). Before use, LPA was dissolved in PBS containing 0.5% fatty acid-free bovine serum albumin (BSA). Protease inhibitor cocktail tablets and BSA were purchased from Roche (Indianapolis, IN). Plasmid DNA was purified using the endo-free purification kit from Qiagen (Valencia, CA). All oligonucleotides were synthesized by Operon Biotechnologies (Huntsville, AL). TRIzol and cell culture medium were obtained from Invitrogen (Carlsbad, CA). Fetal bovine serum (FBS) was from Biomeda (Foster City, CA). Epidermal growth factor (EGF), Ki16425, and anti-flag M_2 and anti-ß-actin monoclonal antibodies were obtained from Sigma (St. Louis, MO). Pertussis toxin (PTX) was purchased from List Biological Laboratories (Campbell, CA). Akt inhibitor II (Akti II) was obtained from Calbiochem (San Diego, CA). Anti-phospho Akt, anti-phospho Erk and anti-tubulin antibodies, and LY294002 were obtained from Cell Signaling (Beverly, MA). The rabbit polyclonal antibody against the C-terminus of the human LPA_4 was kindly provided by Dr. T Shimizu (University of Tokyo).

lpa$_4$ *Targeting Vector*

Similar to the human *lpa*$_4$, the murine *lpa*$_4$ gene is located on the X chromosome in the region 11953246-11969022 (GI no. 51772331). Unlike its intronless human locus (O'Dowd *et al.*, 1997), the mouse *lpa*$_4$ has three exons spanning ~12 kb, whereas the coding sequence is present in exon 3 only (NC_000086). The genomic sequences of the mouse *lpa*$_4$ (C57BL/6) were isolated and PCR amplified from a BAC clone (RP23-343P30; BACPAC Resources, Oakland, CA). A 1.965-kb KpnI/EcoRI fragment containing the 3′ part of exon 3 was PCR amplified from the BAC DNA and cloned as the short arm into the pKO Scrambler NTKV-1901 targeting vector that carries both PGK/*neo*/BGH cassette for positive selection of homologous recombinants with G418 and an MC1-*tk* cassette for negative selection of nonhomologous recombinants with gangcyclovir (Stratagene, La Jolla, CA). The 5.34-kb EcoRI/BstBI fragment containing exon 2 and the major part of intron 2 was cloned into pBluescript II SK(+) from the BAC DNA and recloned using the NotI and SalI sites into the targeting vector. Thus, a 2.591-kb fragment containing the 3′ end of intron 2 and the 5′ portion (with the complete coding sequence) of exon 3 was replaced with 1.603 kb of the PGK/*neo*/BGH cassette, creating the final targeting vector (Figure 1A).

Generating LPA$_4$*-deficinet Mice*

All procedures for animal studies were conducted in compliance with the policies and regulations of Virginia Commonwealth University IACUC. The *lpa*$_4$ targeting vector was linearized with NotI and electroporated into the *129/Sv* embryonic stem (ES) cells HZ2.2 (generated by the VCU Transgenic/Knockout Mouse Core). Genomic DNA from 82 ES cell clones resistant to both G418 and gangcyclovir were screened for homologous recombination by long-range PCR using an *lpa*$_4$ intron 1 sense primer (2717-2740: 5′-CCAAATGTAGGTGCCACTTGTATG-3′) and a PGK antisense primer (5′-GGTGGATGTGGAATGTGTGCGAG-3′) for the long arm, and a *neo* sense primer (5′-TCGCCTTCTTGACGAGTTCTTCTG-3′) and a 3′ flanking antisense primer (12725-12702: 5′-GCCTACAGCCTTATGTATTCCAAC-3′) for the short arm. Southern blot analysis was performed on DNA from these clones using a PGK/*neo*/BGH probe to verify clone purity and the integrity of both genomic arms. Two independent recombinant clones were injected into *C57BL/6* blastocysts, which were then implanted into pseudopregnant *CD-1* recipients, producing two independent lines of chimeric male mice. They were bred with *C57BL/6* females to generate heterozygous female founder mice (X^+X^-) and wild-type (WT) males (X^+Y), which were intercrossed or backcrossed to the male chimeras to generate hemizygous KO males (X^-Y), heterozygous females (X^+X^-), and homozygous KO females (X^-X^-). The WT, heterozygous, and hemizygous mice were further crossed to produce all genotypes summarized in Table 1. Genotypes were determined by PCR amplification of tail genomic DNA (40 cycles of 94°C for 1 min, 60°C for 1 min, and 72°C for 2 min) using a common *lpa*$_4$ intron 2 sense primer (7713-7735: 5′-CTATTGCTTTCCCCCATGTTATG-3′), an *lpa*$_4$ intron 2 antisense primer (8107-8084: 5′-TTACTATTGGCTAGTCTGTCTTTC-3′) for the WT allele, and a PGK antisense primer (5′-GGTGGATGTGGAATGTGTGCGAG-3′) for the KO allele (Figure 1B). Expected sizes of the PCR products for WT and KO alleles were 395 and 564 base pairs, respectively. The lines were subsequently maintained on a mixed *129/Sv* and *C57BL/6* background.

Mouse Embryonic Fibroblasts

Mouse embryonic fibroblasts (MEFs) were isolated from E12.5-13.5 embryos essentially as described (Ishii *et al.*, 2001). The embryos were separated from

Table 1. Inheritance of the *lpa_4* deletion allele

Crossing pairs	Males		Females			Sex ratio (m:f)	Total no. of mice
	X^+Y	X^-Y	X^+X^+	X^+X^-	X^-X^-		
No. of offspring with *lpa_4* genotypes							
$X^+Y \times X^+X^-$	24 (17.4)	36 (26.1)	40 (29.0)	38 (27.5)	0 (0)	60:78 (43.5)	138
$X^-Y \times X^+X^-$	33 (24.8)	29 (21.8)	0 (0)	41 (30.8)	30 (22.6)	62:71 (46.6)	133

Numbers of individual progeny genotyped from the indicated crosses are shown. Values in parentheses are the percentages of the mice with the indicated genotypes or percentages of males vs. the total numbers of mice generated from the indicated crosses (% m/m + f).

the uterine wall and amniotic sac and placed in Petri dishes containing small volumes of PBS. The head and heart tissues were removed. The remaining embryo were minced with surgical scissors and razor blade, digested with 0.25% trypsin/EDTA at 37°C for 25 min, and triturated through a Pasteur pipette. After digestion and removal of undigested tissues, the cells were spun briefly, plated into a 10-cm dish, and allowed to grow to subconfluence in DMEM + 10% FBS. The cells were then either frozen as passage 1 or subcultured at a 1:4 ratio for experiments. Immortalized cell lines were established from primary MEFs using standard protocols for generation of 3T3 cells (Jainchill *et al.*, 1969).

Other Cells

The DLD1 colon cancer cell line was kindly provided by Dr. D. Shida (Virginia Commonwealth University) and maintained as described (Hama *et al.*, 2004). The B103 rat neuroblastoma cell line lacking endogenous LPA receptors was obtained from Dr. J. Chun (Scripps Research Institute) and cultured in DMEM supplemented with 10% FBS, 100 U/ml penicillin, and 100 μg/ml streptomycin (Ishii *et al.*, 2000). The rat hepatoma cell line RH7777 was purchased from ATCC (Manassas, VA) and maintained in the same conditions as B103. These cell lines were frozen at early passages and used for <6 wk in continuous culture.

Fluorescence Microscopy

MEF lines in 60-mm dishes were starved overnight and stimulated with LPA (1 μM) for 30 min. The cells were washed with PBS, fixed with 3% formaldehyde/PBS, and permeabilized with 0.2% Triton X-100 before staining for F-actin with Alexa Fluor 488–labeled phalloidin (1:125 dilution; Invitrogen).

Recombinant Retroviruses and Infection of Cells

The Human LPA_4 or LPA_1 cDNA was inserted between BamHI and XhoI sites upstream of the internal ribosomal entry site of the Moloney murine leukemia retrovirus vector pLZRS-EGFP (a gift of J. Chun, Scripps Research Institute; Ishii *et al.*, 2000). The structure and sequences of the cDNAs in these viral constructs were confirmed by restriction digestion and automatic sequencing. The Bosc23 packaging cell line (ATCC) was transfected with pLZRS-EGFP, pLZRS-EGFP-LPA_4, or pLZRS-EGFP-LPA_1 using Lipofectamine 2000 as described (Invitrogen; Fang *et al.*, 2004). Approximately 20 h after the beginning of transfection, the cells were fed fresh DMEM + 10% FBS. Culture supernatants containing retrovirus were harvested 48 h later, cleared by centrifugation, and used to infect cells or stored at −80°C.

The LPA_1 and LPA_4 cDNAs were also cloned into the pLenti-TOPO lentivirus vector (Invitrogen) as an alternate expression system for LPA receptors. The pLenti-TOPO-LPA_1, pLenti-TOPO-LPA_4 or pLenti-TOPO-LacZ vector was transfected along with packaging plasmids into 293FT cells (Invitrogen) to replicate lentivirus using a protocol similar to that for retrovirus generation in Bosc23 cells. MEF and other cell lines in 35-mm dishes at around 50% confluence were incubated for 16–22 h with 1.5 ml of viral supernatants containing 8 μg/ml polybrene. The infected cells were harvested 72 h after infection. For the cells infected with the retrovirus, EGFP-positive cells were isolated by fluorescence-activated cell sorting (FACS). Lentivirus-infected cells were selected with blasticidin (10 μg/ml) for 10–14 d and pooled colonies were expanded for experiments. When coexpression of LPA_1 and LPA_4 was desired, the recipient cells were infected with the pLenti-TOPO-LPA_1 lentivirus followed by infection with the pLZRS-EGFP-LPA_4 retrovirus.

Western Blot

Cells were lysed in SDS sample buffer or in ice-cold Triton X-100 lysis buffer (1% Triton X-100, 50 mM HEPES, pH 7.4, 150 mM NaCl, 1.5 mM $MgCl_2$, 1 mM EGTA, 10% glycerol, 100 mM NaF, 10 mM Na PPi, and protease inhibitor cocktail). Total cellular proteins were resolved by SDS-PAGE, transferred to Immun-Blot membrane [poly(vinylidene difluoride)]; Bio-Rad, Hercules, CA), and immunoblotted with antibodies following the protocols provided by manufacturers. Immunocomplexes were visualized with an enhanced chemiluminescence detection kit (Amersham, Piscataway, NJ), using horseradish peroxidase–conjugated secondary antibodies (Cell Signaling).

Migration and Invasion Assays

Cell migration was measured in Transwell chambers (pore size 8 μm; BD Biosciences, San Jose, CA; cat. no. 354578). Transwells were coated with 10 μg/ml collagen 1 and placed in the lower chamber containing serum-free DMEM supplemented with LPA or EGF. Cells suspended in serum-free DMEM containing 0.1% fatty acid-free BSA were added to the upper chamber at 2.5×10^4 cells/well or 1.0×10^4 cells/well as indicated. Cells were allowed to migrate for 4 or 6 h at 37°C. Nonmigrated cells were removed from the top filter surface with a cotton swab. Migrated cells attached to the underside of the transwells were washed with PBS and stained with crystal violet and counted under a microscope. The invasion of tumor cells were measured using Transwells coated with growth factor–reduced Matrigel Basement Membrane Matrix (pore size 8 μM; BD Biosciences; cat. no. 354483). The assays were performed as migration assays except that the cells were incubated for 20–24 h before termination of the experiments.

Rho and Rac Activation Assays

Activation of Rho and Rac was analyzed by glutathione *S*-transferase (GST) pulldown assays (Bernard *et al.*, 1999; Ren and Schwartz, 2000). The cells were grown in 10-cm dishes to subconfluence, starved overnight, and stimulated with LPA or vehicle for the indicated periods of time. The cells were lysed in Magnesium-containing lysis buffer (MLB; 25 mM HEPES, pH 7.5, 150 mM NaCl, 1% NP40, 10% glycerol, 10 mM $MgCl_2$, 1 mM EDTA, 1 mM sodium orthovanadate, 10 μg/ml leupeptin, 10 μg/ml aprotinin, and 10 mM NaF). Clarified lysates were incubated for 1 h at 4°C with GST-Rhotekin-RBD (Rho binding domain of Rhotekin, residues 7-89; Ren and Schwartz, 2000) or GST-PAK-PBD (p21 binding domain of PAK, residues 67-150; Bernard *et al.*, 1999) produced in *Escherichia coli* and immobilized on glutathione-coupled Sepharose beads. Beads were washed in MLB three times, eluted with SDS sample buffer, and analyzed by Western blotting using monoclonal anti-Rac antibody (BD Biosciences; cat. no. 610650) or rabbit anti-RhoA antibody (Santa Cruz Biotechnology, SC-418).

Statistics

The γ^2 test of goodness-of-fit was used to determine statistical difference between observed and expected numbers of mice. The null hypothesis is that the number of mice in each category is equal to that predicted by the Mendelian inheritance rule. Numerical results from chemotaxis and invasion experiments were presented as average cell numbers ± SD. The statistical significances of differences were analyzed using Student's *t* test, where $p < 0.05$ was considered significant.

RESULTS

Generation and Characterization of LPA_4-deficient Mice

To determine biological functions of LPA_4, we set out to delete the *lpa_4* gene in mice using the genetic knockout approach. We deleted the 3′ end of intron 2 and 5′ portion of exon 3 that contains the full coding sequences of *lpa_4*, an X chromosome-linked locus (Gene ID: 78134). As detailed in *Materials and Methods*, the chimeric male mice were bred with *C57BL/6* females to generate heterozygous female founder mice (X^+X^-) and WT males (X^+Y), which were further intercrossed to generate hemizygous males (X^-Y). As demonstrated in Table 1, the gender ratios of the offspring [male/(male+female)] from $X^+Y \times X^+X^-$ crossing

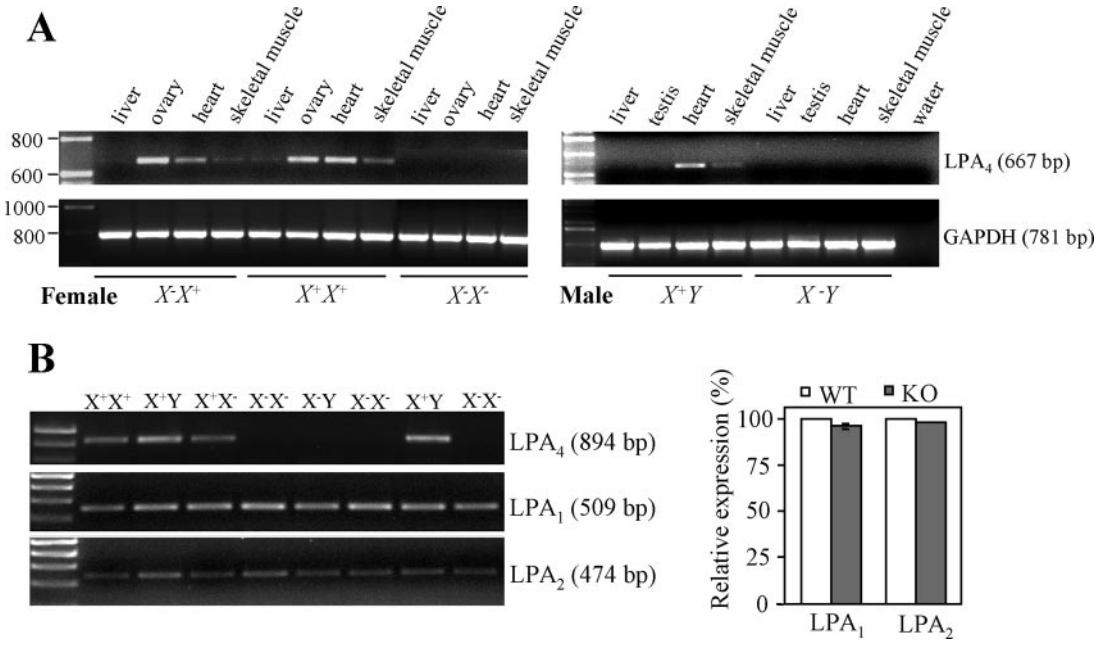

Figure 2. Expression of LPA_4 mRNA in mouse tissues and MEFs. (A) Expression of LPA_4 mRNA in the liver, heart, skeltal muscle, and ovary or testis of female and male adult mice was analyzed by RT-PCR. (B) Expression of LPA_4, LPA_1, and LPA_2 mRNAs in primary MEFs was analyzed by RT-PCR (left). Similar levels of LPA_1 and LPA_2 mRNAs in *lpa*$_4$ WT and KO MEFs were confirmed by RT-qPCR using the Taqman system (ABI; right). The results were normalized on GAPDH and presented as relative percentages with the mRNA levels in WT cells defined as 100%.

and from $X^-Y \times X^+X^-$ crossing were 43.5 and 46.6%, respectively, with an overall percentage of 45.1%, slightly lower than the expected 50%. The differences, however, lacked statistical significance when examined with the γ^2 test of goodness-of-fit. In addition, heterozygous females (X^+X^-), homozygous females (X^-X^-), and hemizygous males (X^-Y) were born at statistically expected Mendelian rule, reflecting that loss of LPA_4 does not cause embryonic lethality or impose a detrimental effect on embryonic development (Table 1). The *lpa*$_4$ KO mice were grossly indistinguishable from their WT or heterozygous littermates in appearance, size, and behavior. They did not show any defects in mating, pregnancy, or litter sizes. There were no gross abnormalities in the internal organs of LPA_4-deficient adults (data not shown).

Expression of LPA$_4$ *in Murine Tissues and MEFs*

To delineate the tissue distribution of LPA_4, we examined its mRNA expression in a number of adult tissues including the liver, heart, skeletal muscle, and ovary or testis. As analyzed by RT-PCR, LPA_4 mRNA was present in the heart, skeletal muscle, and ovary but was seen weakly in the liver or testis (Figure 2A). The expression of LPA_4 mRNA in these tissues was absent from *lpa*$_4$ KO mice.

We isolated MEFs from E12.5 to E13.5 embryos to investigate the impact of LPA_4 deficiency on cellular responses to LPA. RT-PCR analysis showed that WT MEFs expressed transcripts of LPA_1, LPA_2, and LPA_4 (Figure 2B), but lacked LPA_3 or LPA_5 mRNA (data not shown). As expected, no LPA_4 transcript was detected in MEFs from X^-X^- or X^-Y embryos. In addition, deletion of *lpa*$_4$ did not lead to any major compensatory changes in expression levels of LPA_1 or LPA_2 mRNA in MEFs as analyzed by RT-PCR and confirmed by RT-quantitative (q)PCR (Figure 2B).

Enhancement of Migratory Response to LPA by lpa$_4$ *Deletion*

Previous studies using MEFs from *lpa*$_1$ and *lpa*$_2$ double knockouts revealed relative contributions of each of these receptors to activation of intracellular signaling cascades by LPA (Contos *et al.*, 2002). Furthermore, analysis of $lpa_1^{-/-}$ fibroblasts provided compelling evidence that the LPA_1 receptor was the most critical mediator of the migratory response to LPA in these cells (Hama *et al.*, 2004).

Both LPA_4-negative and WT MEFs showed morphological characteristics of fibroblasts (Figure 3A). However, LPA_4-deficient MEFs exhibited an apparently more flattened shape distinguishable from WT MEFs, which were more heterogeneous in size and shape (Figure 3, A and B). Because morphology and migratory potential of mammalian cells are closely associated and coordinately regulated by Rho GTPases (Nobes and Hall, 1999; Van Leeuwen *et al.*, 2003; Yanagida *et al.*, 2007), we examined whether lack of LPA_4 affects migratory response to LPA. We compared WT and LPA_4-negative MEFs for LPA-induced cell migration using the transwell chambers. Surprisingly, the LPA_4-deficient MEFs exhibited remarkably enhanced migratory response to LPA (Figure 3C) compared with WT cells that only weakly responded to LPA. Consistent with this difference in cell migration, LPA stimulated lamellipodia formation in more LPA_4-deficient cells than WT control cells (Figure 3B). Of interest, the LPA_4-deficient MEFs were also more motile than WT MEFs in unstimulated conditions (Figure 3C), suggesting that some endogenous LPA may exist or accumulate in the cellular microenvironment during the course of the experiments. Consistent with the greater basal migratory potential associated with loss of LPA_4, more *lpa*$_4$ KO MEFs than WT cells migrated toward EGF (Figure 3C). However, the net increase by EGF over unstimulated conditions was similar between *lpa*$_4$ KO and WT MEFs. Thus lack of LPA_4

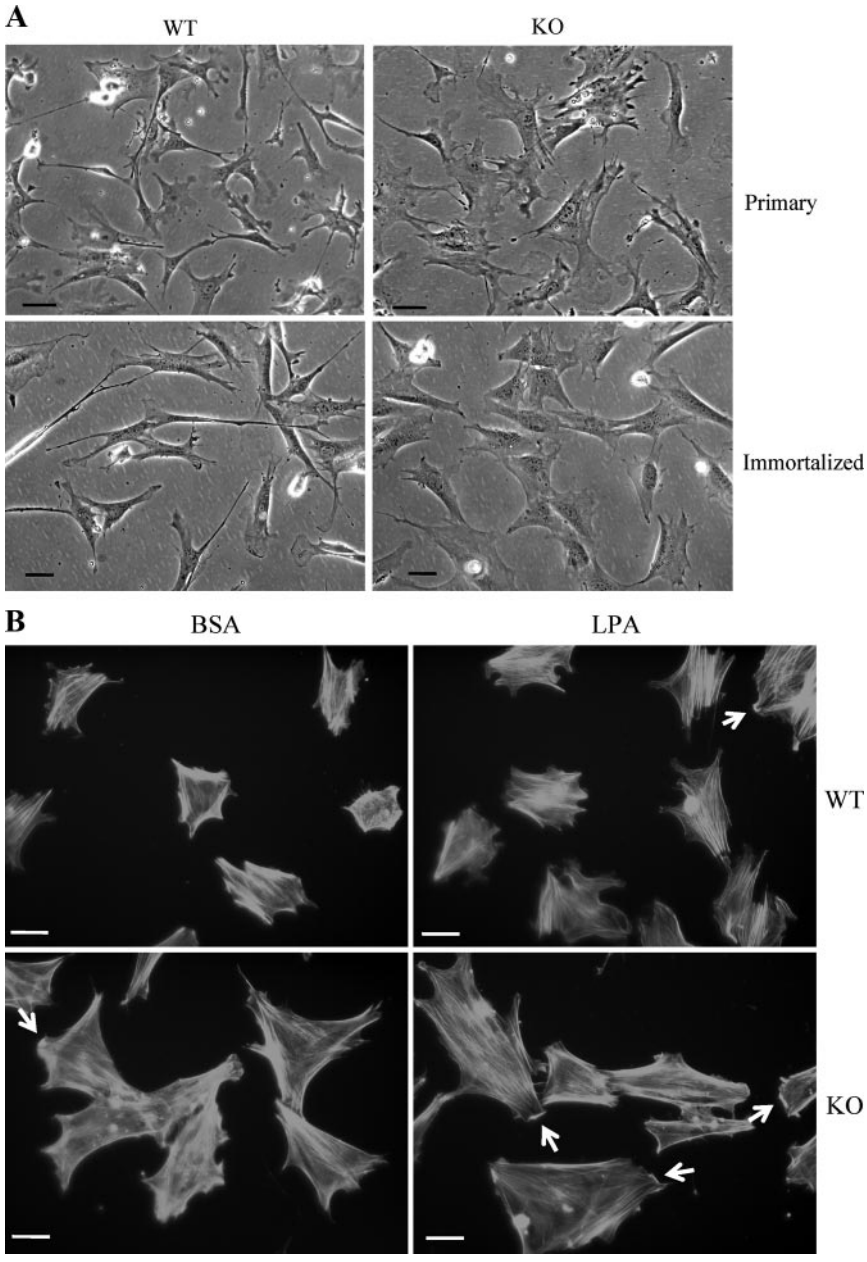

Figure 3. Sensitization of LPA_4-deficient MEFs to migratory response to LPA. (A) *lpa_4* KO MEFs showed a more flattened morphology compared with the WT counterparts. Shown were microscopic photographs of primary MEFs (top panels) and immortalized MEF lines (bottom panels). Bar, 30 μm. (B) LPA-induced lamellipodium formation in WT and *lpa4* KO MEFs. The cells were stimulated with or without LPA (1 μM) for 30 min and stained with Alexa Fluor 488–labeled phalloidin as described in *Materials and Methods.* More lamellipodium formation (arrows) was observed in LPA-stimulated KO MEFs than in WT MEFs. Bar, 30 μm.

specifically sensitized MEFs to LPA-induced cell migration. Furthermore, the enhancement of LPA-mediated cell migration in the absence of LPA_4 was consistent among multiple pairs of LPA_4 WT and KO MEFs (data not shown) and was observed in both primary MEFs and immortalized MEF lines (Figure 3C).

Potentiation of Akt and Rac Activation by lpa_4 Deletion

To understand functions of *lpa_4* in cell signaling, we analyzed activation of Akt and Erk by LPA in WT and *lpa_4* KO MEFs. Although LPA-induced Erk phosphorylation was similar between WT and KO MEFs, LPA_4 deficiency resulted in enhancement of Akt phosphorylation at Thr-308 in response to LPA (Figure 3D). The potentiating effect of LPA_4 deficiency on Akt activation was seen in multiple pairs of WT and KO MEFs (data not shown). Furthermore, the enhanced Akt activation in LPA_4-deficient cells was sensitive to LPA_1-selective antagonist Ki16425 (Ohta *et al.*, 2003), the Gi inhibitor PTX, and the PI3K inhibitor LY294002 (Figure 3D), indicating that the prominent Akt activation was mediated through the LPA_1-Gi-PI3K signaling route in LPA_4-deficient cells. Moreover, LPA-induced migration of LPA_4-deficient cells was suppressed by Ki16425, PTX, or LY294002 but only slightly reduced by an Akt inhibitor (Akti II; Kozikowski *et al.*, 2003), suggesting that an LPA_1-Gi-PI3K–dependent pathway mediates the robust migratory response to LPA in LPA_4-deficeint cells.

We next examined LPA-induced activation of Rac, a well-documented effector of PI3K, and the G12/13 downstream target Rho (van Leeuwen *et al.*, 2003; van Meeteren and Moolenaar, 2007; Yanagida *et al.*, 2007). Rac and Rho mediate cell migration in a coordinate manner. Rac promotes lamellipodia protrusion and forward movement, whereas RhoA regulates actomyosin-driven cytoskeleton contraction and

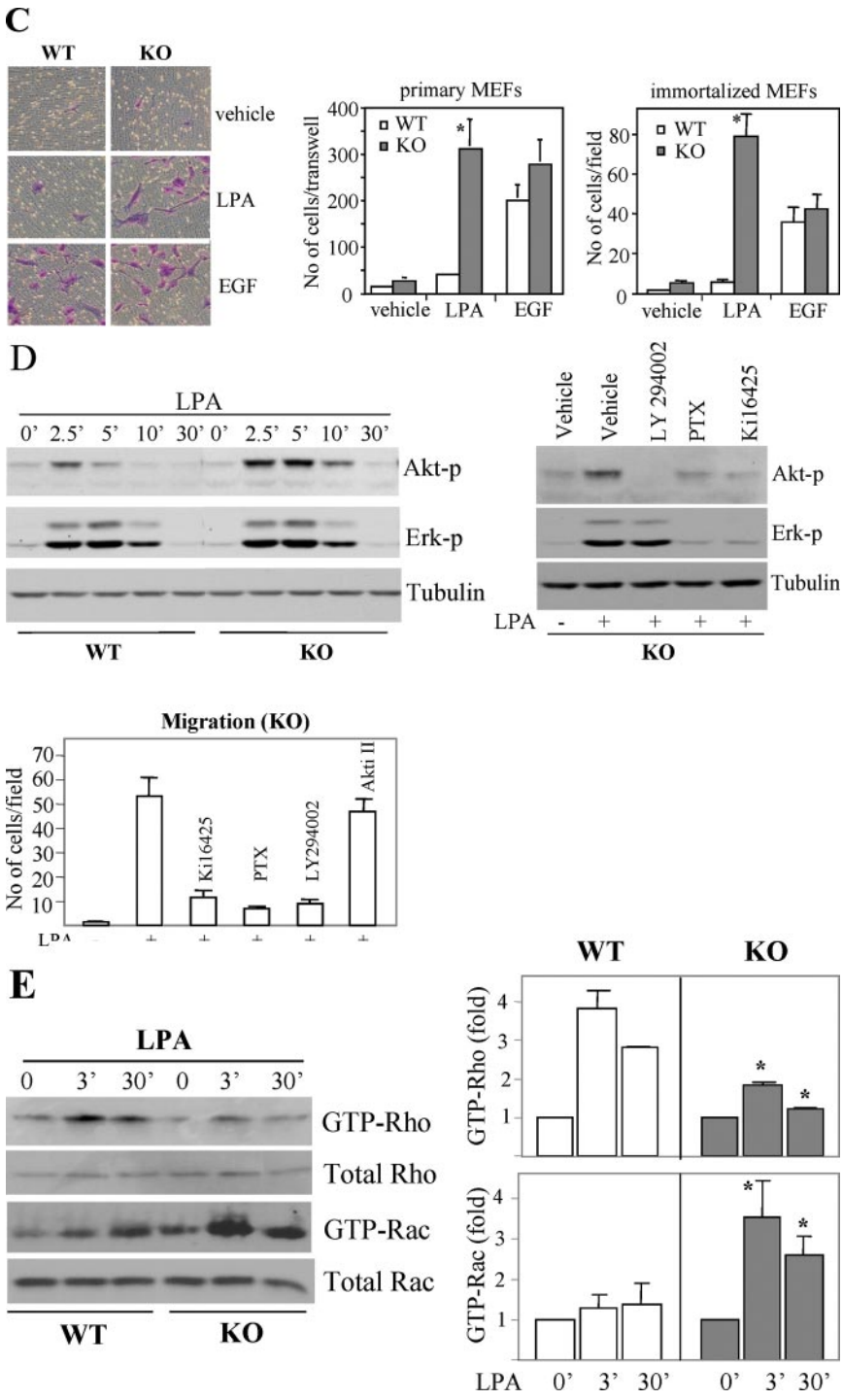

Figure 3 (cont). (C) LPA_4-deficient MEFs were hypersensitive to LPA-induced migration. The migratory response to LPA (5 μM) or EGF (25 ng/ml) in primary WT and KO MEFs were analyzed using transwells. The cells (2.5×10^4 cells/0.5 ml) were loaded to the upper wells and allowed to migrate for 6 h. The migrated cells on the underside of transwells were stained with crystal violet and photographed under microscope (200×; left). The migratory responses to LPA and EGF in both primary MEFs and immortalized MEF lines were quantified (right). Results were average numbers of migrated cells per transwell (primary MEFs) or per field (immortalized MEFs) from triplicate transwells (mean ± SD). The number of migrated cells/field were determined by counting at least five randomly selected fields from each transwell (200× magnification). The data shown was representative of three independent experiments. (D) LPA_4 deficiency sensitizes MEFs to LPA-induced Akt activation. The WT and KO MEF lines were starved in serum-free medium and stimulated with LPA (2.5 μM) for the indicated time periods (top left) or in the presence of the LPA_1 antagonist Ki16425 (10 μM), Gi inhibitor PTX (50 ng/ml), or PI3K inhibitor LY294002 (10 μM; top right). Phosphorylation of Akt at Thr308 and Erk at Thr202/Tyr204 of Erk1 and Thr185/Tyr187 of Erk2 were analyzed by immunoblotting with Akt and Erk phospho-specific antibodies. LPA-induced chemotaxis in the KO MEF line was quantified in the absence or presence of the indicated inhibitors or Akt inhibitor (Akti II; 10 μM). (E) LPA_4 deficiency decreases Rho but potentiates Rac activation by LPA. WT and KO MEF lines were stimulated with LPA (2.5 μM) for the indicated periods of time and analyzed for GTP-bound Rac or Rho with the GST pulldown assays as described in *Materials and Methods*. The GTP-Rho and GTP-Rac levels in control and LPA-stimulated cells in three independent experiments were quantified by densitometry and presented as fold change relative to the values in unstimulated cells (defined as 1; right panel). The statistical significances of differences at 3 or 30 min after LPA stimulation between WT and KO MEFs were indicated with asterisks ($p < 0.05$).

detachment of the rear of migrating cells (Nobes and Hall, 1999). LPA-induced Rac activation in fibroblasts is generally weak and has been best demonstrated in LPA receptor-overexpressing cells (van Leeuwen *et al.*, 2003; Pilquil *et al.*, 2006). As shown in Figure 3E, Rac activation in response to LPA was barely detectable in WT MEFs, which correlated with the weak migratory response to LPA in WT cells. In contrast, LPA evoked prominent increases in Rac-GTP levels in the *lpa*$_4$ KO MEFs (Figure 3E).

In contrast to Rac activation, LPA-induced Rho activation was oppositely affected by LPA_4 deficiency. As shown in Figure 3E, LPA induced immediate and sustained increases in Rho-GTP levels in both WT and *lpa*$_4$ KO MEFs as measured by pulldown with GST-Rhotekin Sepharose beads. However, the magnitude of Rho activation induced by LPA was significantly reduced in *lpa*$_4$ KO cells, suggesting that signaling through LPA_4 contributes to the overall Rho activation in LPA-stimulated cells. The result was consistent with the previous observation that in skin fibroblasts of LPA_1 and LPA_2 double knockouts, LPA remained capable of stimulating partial activation of Rho (Hama *et al.*, 2004), which could be attributed to the input of the LPA_4 receptor.

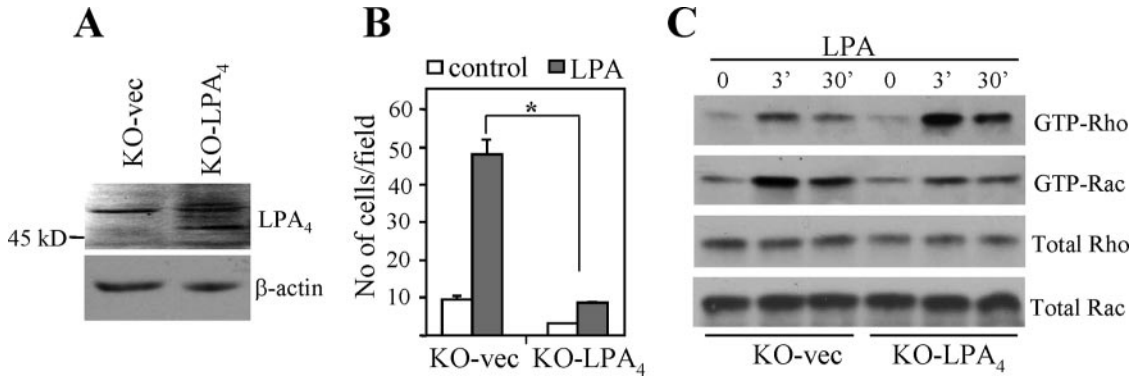

Figure 4. Desensitization of LPA_4-deficienct cells to LPA-induced migration by reconstitution of LPA_4. (A) LPA_4 expression was reconstituted in KO MEF line by infection with pLenti-LPA_4 lentivirus. The expression of LPA_4 in transduced cells (KO-LPA_4) but not in control virus-infected cells (KO-vec) was confirmed by immunoblotting with an anti-LPA_4 antibody. (B) The migratory response to LPA in these cells was quantified as described in Figure 3. (C) Reexpression of LPA_4 enhanced Rho but decreased Rac activation induced by LPA. Rho and Rac activation was analyzed with the GST pulldown assays as in Figure 3. Similar results were obtained from two independent experiments.

Inhibition of Cell Motility by Reconstitution of LPA_4

To verify the critical role for LPA_4 in restraining Rac activation and cell migration induced by LPA, we infected an LPA_4-negative MEF line with LPA_4-lentivirus to reconstitute LPA_4 expression (Figure 4A). The LPA-induced migration in control virus-infected and LPA_4-reconstituted cells was compared. As shown in Figure 4B, LPA_4-reexpressing cells migrated in response to LPA less efficiently than the control virus-infected, LPA_4-negative cells, confirming that LPA_4 functions as a suppressor of LPA-dependent cell migration. Furthermore, the inhibition of LPA-dependent cell migration by reexpression of LPA_4 was accompanied by increased Rho but decreased Rac activation induced by LPA (Figure 4C).

Suppression of LPA-induced Cell Migration and Invasion by LPA_4 in Colon Cancer Cells

To explore the physiological significance of the motility inhibitory effect of LPA_4, we assessed the role of LPA_4 in the control of migration and invasion of human cancer cells. The DLD1 colon cancer cell line was previously shown to migrate efficiently in response to LPA (Shida *et al.,* 2003). Submicromolar concentrations of LPA were sufficient to trigger significant migratory response to LPA in DLD1 cells. DLD1 cells expressed LPA_1 and LPA_2, but lacked LPA_3 or LPA_4 mRNA as analyzed by RT-qPCR (Figure 5A). We introduced LPA_4 into DLD1 cells via lentivirus-mediated transduction (Figure 5B). LPA-, but not EGF-induced migration in DLD1 cells was dramatically inhibited by ectopic expression of LPA_4 (Figure 5C). LPA was also effective in stimulating invasion of DLD1 cells through the Matrigel Basement Membrane Matrix. The invasion induced by LPA was similarly suppressed by expression of LPA_4 (Figure 5C). The inhibitory effect of LPA_4 on migration and invasion of DLD1cells was not due to interference with endogenous LPA_1 or LPA_2 receptor expression. In fact, after introduction of LPA_4, LPA_2 mRNA expression was not altered and LPA_1 mRNA level was modestly increased as determined by RT-qPCR (Figure 5B). Collectively, these results establish a general role for LPA_4 in negative regulation of motility-stimulating activity of LPA in both normal and neoplastic cells.

Antagonism of LPA_1-dependent Cell Migration by LPA_4

Most mammalian cell types express more than one LPA receptor subtype and respond to LPA, making it difficult to connect a cellular response to a specific LPA receptor. It is of interest to study cooperative or antagonistic interactions among LPA receptor subtypes. The rat neuroblastoma cell line B103 offers an ideal model to examine the receptor cross-talk due to the absence of endogenous LPA receptors (Ishii *et al.,* 2000). Although it was recently shown that there was slight expression of LPA_4 mRNA in B103 cells, the cell line did not respond to LPA stimulation (Yanagida *et al.,* 2007). Therefore, we infected B103 with retrovirus carrying LPA_4 or LPA_1, or with control retrovirus. The transduced, GFP-positive cells were isolated by FACS and expanded as stable lines expressing LPA_4 or LPA_1. In agreement with LPA_4 being a functional receptor for LPA, LPA_4-expressing B103 cells underwent neurite retraction and cell rounding upon exposure to LPA (Figure 6A), similar to the response seen in LPA_1-expressing B103 cells. However, only LPA_1-expressing cells showed chemotactic response to LPA, whereas the LPA_4-expressing cells and vector control cells did not (Figure 6A). The observation indicates that LPA_4 is not capable of driving cell migration in spite of its ability to promote Rho-dependent neurite retraction.

To determine whether LPA_4 counteracts the motility-stimulating action of LPA_1, we coexpressed LPA_1 and LPA_4 in B103 cells by sequential infection with pLenti-TOPO-LPA_1 lentivirus and pLZRS-EGFP-LPA_4 retrovirus. Coexpression of these LPA receptors was confirmed by Western blotting (Figure 6B). Interestingly, LPA_4 expression indeed inhibited LPA_1-mediated migration of B103 cells induced by LPA. The LPA_1-dependent migration was inhibited by coexpressed LPA_4 by 40%, not as strongly as seen in LPA_4-reexpressing MEFs or LPA_4-transduced DLD1 cells probably because the coexpressed LPA_1 receptor was abundant in the recipient cells (Figure 6B). High levels of LPA_1 could provide a strong motility-promoting drive upon LPA stimulation. In addition, B103 cells expressing LPA_1 was capable of invading through Matrigel in response to LPA. This effect was also significantly attenuated in the cells co-expressing LPA_4 (Figure 6B).

DISCUSSION

LPA has been a subject of extensive research in signal transduction and physiology. Six GPCRs have been identified as cognate LPA receptors to mediate a multitude of cellular responses to LPA (Hecht *et al.,* 1996; An *et al.,*1998; Bandoh

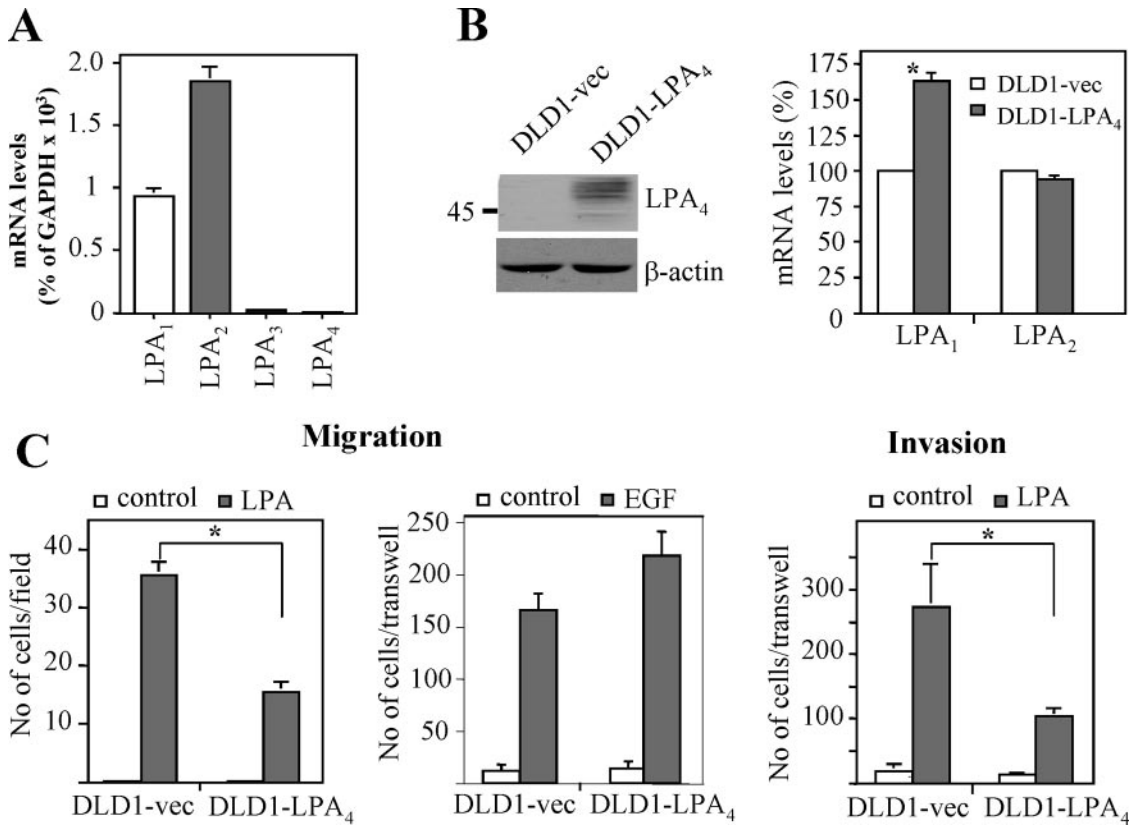

Figure 5. Inhibition of LPA-induced migration and invasion of the DLD1 colon cancer cells by LPA_4. (A) RT-qPCR analysis indicated expression of LPA_1 and LPA_2 but not LPA_3 or LPA_4 mRNA in DLD1 cells. The mRNA levels were presented as percentages relative to GAPDH. (B) Ectopic expression of LPA_4 did not decrease expression of motility-promoting Edg LPA receptors. Immunoblotting analysis confirmed the expression of transduced LPA_4 in DLD1-LPA_4 cells (left). Expression levels of endogenous LPA_1 and LPA_2 mRNAs in DLD1-vec and DLD1-LPA_4 cells were compared by RT-qPCR. Right, the results were normalized on GAPDH and presented as relative percentages with the mRNA levels in the control DLD1-vec cells defined as 100%. (C) Expression of LPA_4 inhibited LPA- but not EGF-induced cell motility. The DLD1-vec and DLD1-LPA_4 cells (2.5×10^4 cells/transwell, 0.2 μM LPA or 25 ng/ml EGF) were allowed to migrate for 6 h or to invade through Matrigel for 24 h. The cell numbers, LPA concentrations and incubation times used in the experiments were determined empirically that yielded maximal or submaximal responses. The results of migration and invasion assays were presented as detailed in Figure 3.

et al., 1999; Im *et al.*, 2000; Noguchi *et al.*, 2003; Lee *et al.*, 2006; Pasternack *et al.*, 2008). It remains elusive why there are multiple receptor subtypes of two distant families for the small lipid mediator. The LPA_4 receptor is linked to Gq, G12/13 and probably Gs, but not Gi, whereas LPA_{1-3} receptors all couple to Gi (Hecht *et al.*, 1996; An *et al.*, 1998; Bandoh *et al.*, 1999; Im *et al.*, 2000; Noguchi *et al.*, 2003; Lee *et al.*, 2006). The differences in receptor structure and G protein partnership between the Edg LPA receptors and the LPA_4 receptor prompted us to study biological functions of LPA_4 by developing knockout mice. Although the interim characterization has not revealed apparent abnormalities in LPA_4-deficient mice, the truly LPA_4-negative MEFs isolated from LPA_4-deficient embryos have allowed us to evaluate the role of LPA_4 in LPA signal transduction and migratory response to LPA. The results presented in the current work clearly demonstrate that knockout of LPA_4 sensitizes the cells to LPA-induced migration. In WT cells, the presence of LPA_4 may thus serve as a barrier preventing overreaction to LPA. The specific role of LPA_4 in limiting LPA-induced cell motility was confirmed by LPA_4 reconstitution experiment showing reexpression of LPA_4 desensitizes KO MEFs to LPA-induced migration. Moreover, heterologous expression of LPA_4 in rat neuroblastoma and human colon cancer cell lines suppressed LPA-triggered cell migration and invasion, antagonizing the motility-promoting effect of the LPA_1 receptor. It will be of interest to examine in the future whether LPA_4 expression was deregulated in human tumors contributing to the invasive and metastatic potential of cancer cells.

The discovery of negative regulation of LPA-dependent migration by LPA_4 provides novel insights into the cross-talk among the multiple LPA receptors that are frequently coexpressed in mammalian cells. We have recently described that LPA induced cyclooxygenase-2 expression in ovarian cancer cells through a mechanism requiring LPA_1, LPA_2, and LPA_5 receptors (Oyesanya *et al.*, 2008). Integration of signals from multiple LPA receptors may be necessary for the optimal activation of LPA-mediated responses. There are many other examples of functional complementation or redundancy among LPA receptors (Ishii *et al.*, 2000; Fang *et al.*, 2004; Lin *et al.*, 2007; Oyesanya *et al.*, 2008). However, the functional antagonism between LPA receptors has rarely been demonstrated (Ishii *et al.*, 2000). The opposing effects of LPA_1 and LPA_4 receptors on LPA-induced cell migration and invasion described in the current work represent such an example of functional inhibition among LPA receptors. This inhibitory cross-talk is likely critical to ensure physiologically appropriate responses to LPA. It is yet to be determined whether LPA_4 also negatively regulate some other biological functions of LPA. In B103 cells, LPA_4 mimics

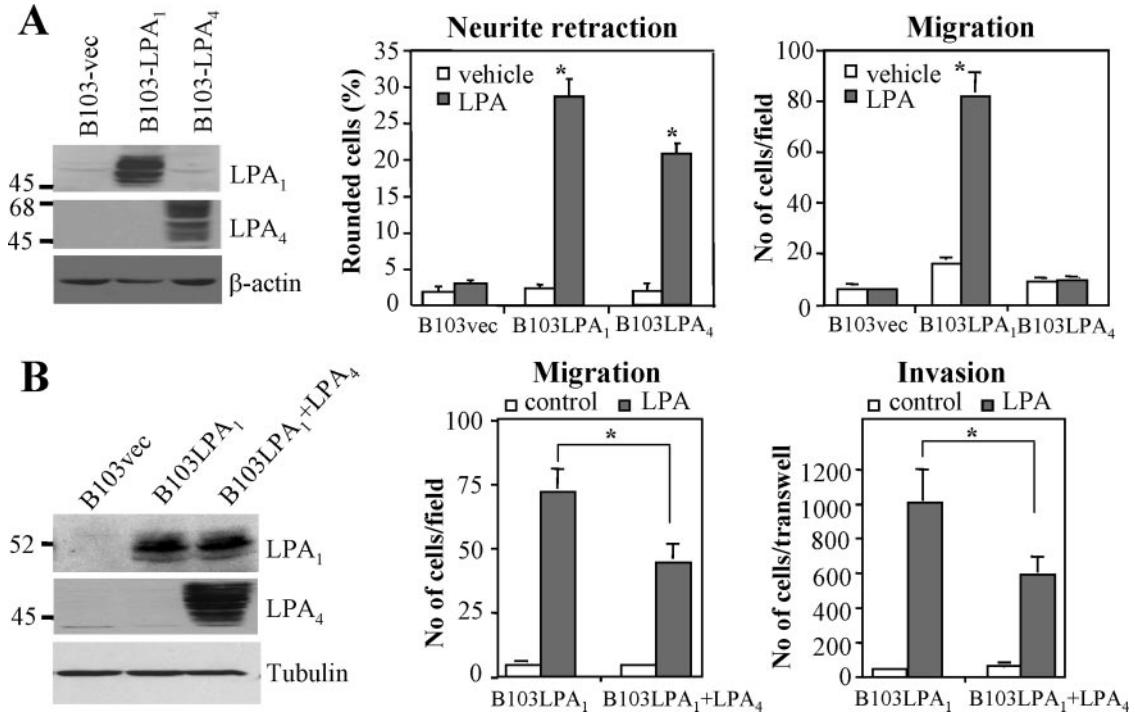

Figure 6. Antagonism of LPA_1-dependent cell migration by LPA_4. (A) LPA_4 was capable of mediating neurite retraction but not migratory response to LPA. Expression of transduced LPA_1 or LPA_4 proteins in the respective cells was analyzed by immunoblotting (left panel). LPA-induced neurite retraction and cell migration in vector control, LPA_1- or LPA_4-expressing cells were analyzed (right panels). For neurite retraction, the cells were plated in six-well plates coated with 0.01% poly-L-lysine at 5×10^4 cells/well. The next day, the cells were starved overnight and stimulated with LPA (1 μM) or vehicle (BSA) for 15 min. Percentages of rounded cells showing neurites shorter than the cell body were calculated based on the total numbers of cells. For analysis of migratory response to LPA (1 μM), the cells (1×10^4 cells/0.5 ml) were allowed to migrate for 4 h. The results presented were average numbers of cells/field (200×) ± SD of triplicates. (B) LPA_4 inhibited LPA_1-mediated migration and invasion when coexpressed with LPA_1. B103 cells were transduced with vector (B103-vec), LPA_1 (B103-LPA_1), or both LPA_1 and LPA_4 (B103-LPA_1 + LPA_4; right panel). The chemotactic migration induced by LPA in these cells was analyzed under the same conditions as in A (middle panel). The in vitro invasion assays were performed with LPA (1 μM) and 1×10^4 cells/transwell coated with Matrigel as described in Figure 5 (right panel).

LPA_1 in promoting neurite retraction and cell rounding, suggesting that LPA_4 is indeed a functional LPA receptor that mediates certain cellular effects of LPA while inhibiting others, depending on signaling pathways involved.

Although the molecular mechanism for LPA_4 down-regulation of cell motility remains to be fully elucidated, our results provide some clues to the potential players in the process. As discussed above, the cell motility is tightly controlled by activities of Rho and Rac in a coordinate manner (Nobes and Hall, 1999). The balance of Rho and Rac activities are critical determinants of cell movement (Nobes and Hall, 1999). LPA_4 contributes to the total Rho activation in MEFs likely through G12/13 (Noguchi *et al.*, 2003). Our results demonstrate that loss of LPA_4 decreased LPA-stimulated Rho activation as anticipated but simultaneously enhanced LPA-induced Rac activation. The observation suggests that LPA_4 may exert its inhibitory effect on cell migration through increasing the relative ratios of active Rho versus active Rac in LPA-treated cells. LPA_4 seems to interfere with activation of Rac by inhibiting PI3K. This is supported by the fact that LPA_4 expression attenuates other PI3K effectors such as Akt. In addition to this possibility, Rac activation could be inhibited by excessive Rho activity in WT cells as has been proposed in other cell systems (Arikawa *et al.*, 2003; Sugimoto *et al.*, 2003, 2006). It is also possible that LPA_4 directly desensitizes the LPA_1 receptor that is known to stimulate Rac activation through Gi (van Leeuwen *et al.*, 2003). The role of LPA_4 in negative control of cell motility is reminiscent of $S1P_2$, one of S1P receptors, that has been shown to inhibit cell migration (Arikawa *et al.*, 2003; Sugimoto *et al.*, 2003). Similar to LPA_4, $S1P_2$ is coupled to G12/13 and Gq, but not Gi (Arikawa *et al.*, 2003; Sugimoto *et al.*, 2003). Several studies suggest the negative effect of $S1P_2$ on cell motility is attributed to G12/13-mediated Rho activation (Arikawa *et al.*, 2003; Sugimoto *et al.*, 2003). Activation of Rho in the absence of appropriate Rac input seems to be sufficient to confer inhibition of cell motility (Arikawa *et al.*, 2003; Sugimoto *et al.*, 2003, 2006).

It is not surprising that the LPA_4-deficient mice do not show obvious phenotypic abnormalities at least at early ages. LPA_1 and LPA_2 knockouts are also dispensable from normal development and physiology (Contos *et al.*, 2000, 2002). However, these knockout animals have proved to be valued models to link LPA signaling to pathophysiological processes (Inoue *et al.*, 2004; Pradere *et al.*, 2007; Tager *et al.*, 2008). The backup and/or redundant receptor subtypes of LPA may suffice to compensate for the loss of individual LPA receptors in vivo. Alternatively, LPA, as one of phospholipids present in the circulation and tissues, may not be the only or rate-limiting mediator physiologically required in vivo. Instead, LPA signaling may be more critical in pathophysiological settings when levels of the lipid mediator are locally and temporally altered. Recent studies of LPA_1-deficeint mice demonstrated involvement of LPA_1 in abnormal wound healing and fibrosis formation (Pradere *et al.*, 2007; Tager *et al.*, 2008), supporting a major role for this

LPA receptor subtype in chemotactic recruitment of fibroblasts to the site of wound. In light of the opposing effects of LPA_4 and LPA_1 on migratory response of various cell types to LPA, it is interesting to study roles of LPA_4 in wound healing and other pathophysiological conditions using LPA_4-deficient mice developed in the current study.

ACKNOWLEDGMENTS

The authors thank Dr. T. Shimizu (University of Tokyo) for providing an antibody against LPA_4, Dr. J. Chun (Scripps Research Institute) for B103 cells and the pLZRS-EGFP retrovirus vector, and Dr. K Lynch (University of Virginia) for LPA_4 cDNA. The work has been supported in part by the National Institutes of Health (NIH), National Cancer Institute Grant CA102196 (X.F.), the Department of Defense career development award W81XWH0410103 (X.F.), the Massey Cancer Center pilot project grant (X.F.), and the NIH Grant P30 CA016059 funds to the Massey Cancer Center/VCU Transgenic/Knockout Mouse Shared Resource.

REFERENCES

An, S., Bleu, T., Hallmark, O. G., and Goetzl, E. J. (1998). Characterization of a novel subtype of human G protein-coupled receptor for lysophosphatidic acid. J. Biol. Chem. *273*, 7906–7910.

Arikawa, K., Takuwa, N., Yamaguchi, H., Naotoshi, S., Joji, K., Hirokazu, N., Kazuhiko, T., and Yoh, T. (2003). Ligand-dependent inhibition of B16 melanoma cell migration and invasion via endogenous S1P2 G protein-coupled receptor: Requirement of inhibition of cellular RAC activity. J. Biol. Chem. *278*, 32841–32851.

Bandoh, K., Aoki, J., Hosono, H., Kobayashi, S., Kobayashi, T., Murakami-Murofushi, K., Tsujimoto, M., Arai, H., and Inoue, K. (1999). Molecular cloning and characterization of a novel human G-protein-coupled receptor, EDG7, for lysophosphatidic acid. J. Biol. Chem. *274*, 27776–27785.

Benard, V., Bohl, B. P., and Bokoch, G. M. (1999). Characterization of rac and cdc42 activation in chemoattractant-stimulated human neutrophils using a novel assay for active GTPases. J. Biol. Chem. *274*, 13198–13204.

Chan, L. C., Peters, W., Xu, Y., Chun, J., Farese, R. V., Jr., and Cases, S. (2007). LPA3 receptor mediates chemotaxis of immature murine dendritic cells to unsaturated lysophosphatidic acid (LPA). J. Leukoc. Biol. *82*, 1193–1200.

Chen, M., Towers, L. N., and O'Connor, K. L. (2007). LPA2 (EDG4) mediates rho-dependent chemotaxis with lower efficacy than LPA1 (EDG2) in breast carcinoma cells. Am. J. Physiol. Cell Physiol. *292*, C1927–C1933.

Contos, J. J., Fukushima, N., Weiner, J. A., Kaushal, D., and Chun, J. (2000). Requirement for the lpA1 lysophosphatidic acid receptor gene in normal suckling behavior. Proc. Natl. Acad. Sci. USA *97*, 13384–13389.

Contos, J. J., Ishii, I., Fukushima, N., Kingsbury, M. A., Ye, X., Kawamura, S., Brown, J. H., and Chun, J. (2002). Characterization of lpa(2) (Edg4) and lpa(1)/lpa(2) (Edg2/Edg4) lysophosphatidic acid receptor knockout mice: signaling deficits without obvious phenotypic abnormality attributable to lpa(2). Mol. Cell. Biol. *22*, 6921–6929.

Eichholtz, T., Jalink, K., Fahrenfort, I., and Moolenaar, W. H. (1993). The bioactive phospholipid lysophosphatidic acid is released from activated platelets. Biochem. J. *291*, 677–680.

Fang, X. *et al.*. (2004). Mechanisms for lysophosphatidic acid-induced cytokine production in ovarian cancer cells. J. Biol. Chem. *279*, 9653–9661.

Hama, K. *et al.* (2004). Lysophosphatidic acid and autotaxin stimulate cell motility of neoplastic and non-neoplastic cells through LPA1. J. Biol. Chem. *279*, 17634–17639.

Hecht, J. H., Weiner, J. A., Post, S. R., and Chun, J. (1996). Ventricular zone gene-1 (vzg-1) encodes a lysophosphatidic acid receptor expressed in neurogenic regions of the developing cerebral cortex. J. Cell Biol. *135*, 1071–1083.

Howe, L. R., and Marshall, C. J. (1993). Lysophosphatidic acid stimulates mitogen-activated protein kinase activation via a G-protein-coupled pathway requiring p21ras and p74raf-1. J. Biol. Chem. *268*, 20717–20720.

Im, D. S., Heise, C. E., Harding, M. A., George, S. R., O'Dowd, B. F., Theodorescu, D., and Lynch, K. R. (2000). Molecular cloning and characterization of a lysophosphatidic acid receptor, Edg-7, expressed in prostate. Mol. Pharmacol. *57*, 753–759.

Inoue, M., Rashid, M. H., Fujita, R., Contos, J. J., Chun, J., and Ueda, H. (2004). Initiation of neuropathic pain requires lysophosphatidic acid receptor signaling. Nat. Med. *10*, 712–718.

Ishii, I., Contos, J. J., Fukushima, N., and Chun, J. (2000). Functional comparisons of the lysophosphatidic acid receptors, LP(A1)/VZG-1/EDG-2, LP(A2)/EDG-4, and LP(A3)/EDG-7 in neuronal cell lines using a retrovirus expression system. Mol. Pharmacol. *58*, 895–902.

Ishii, I., Friedman, B., Ye, X., Kawamura, S., McGiffert, C., Contos, J. J., Kingsbury, M. A., Zhang, G., Brown, J. H., and Chun, J. (2001). Selective loss of sphingosine 1-phosphate signaling with no obvious phenotypic abnormality in mice lacking its G protein-coupled receptor, LP(B3)/EDG-3. J. Biol. Chem. *276*, 33697–33704.

Jainchill, J. L., Aaronson, S. A., and Todaro, G. J. (1969). Murine sarcoma and leukemia viruses: assay using clonal lines of contact-inhibited mouse cells. J. Virol. *4*, 549–553.

Kozikowski, A. P., Sun, H., Brognard, J., and Dennis, P. A. (2003). Novel PI analogues selectively block activation of the pro-survival serine/threonine kinase Akt. J. Am. Chem. Soc. *125*, 1144–1145.

Lee, C. W., Rivera, R., Gardell, S., Dubin, A. E., and Chun, J. (2006). GPR92 as a new G12/13- and Gq-coupled lysophosphatidic acid receptor that increases cAMP, LPA5. J. Biol. Chem. *281*, 23589–23597.

Lin, C. I., Chen, C. N., Lin, P. W., Chang, K. J., Hsieh, F. J., and Lee, H. (2007). Lysophosphatidic acid regulates inflammation-related genes in human endothelial cells through LPA1 and LPA3. Biochem. Biophys. Res. Commun. *363*, 1001–1008.

McIntyre, T. M. *et al.* (2003). Identification of an intracellular receptor for lysophosphatidic acid (LPA): LPA is a transcellular PPARgamma agonist. Proc. Natl. Acad. Sci. USA *100*, 131–136.

Mills, G. B., and Moolenaar, W. H. (2003). The emerging role of lysophosphatidic acid in cancer. Nat. Rev. Cancer *3*, 582–591.

Nobes, C. D., and Hall, A. (1999). Rho GTPases control polarity, protrusion, and adhesion during cell movement. J. Cell Biol. *144*, 1235–1244.

Noguchi, K., Ishii, S., and Shimizu, T. (2003). Identification of p2y9/GPR23 as a novel G protein-coupled receptor for lysophosphatidic acid, structurally distant from the edg family. J. Biol. Chem. *278*, 25600–25606.

O'Dowd, B. F., Nguyen, T., Jung, B. P., Marchese, A., Cheng, R., Heng, H. H., Kolakowski, L. F., Jr., Lynch, K. R., and George, S. R. (1997). Cloning and chromosomal mapping of four putative novel human G-protein-coupled receptor genes. Gene *187*, 75–81.

Ohta, H. *et al.* (2003). Ki16425, a subtype-selective antagonist for EDG-family lysophosphatidic acid receptors. Mol. Pharmacol. *64*, 994–1005.

Oyesanya, R. A., Lee, Z., Wu, J., Chen, J., Song, Y., Mukherjee, A., Dent, P., Kordula, T., Zhou, H., and Fang, X. (2008). Transcriptional and post-transcriptional mechanisms for lysophosphatidic acid-induced cycloxygenase expression in ovarian cancer cells. FASEB J. *22*, 2639–2651.

Pasternack, S. M. *et al.* (2008). G protein-coupled receptor P2Y5 and its ligand LPA are involved in maintenance of human hair growth. Nat. Genet. *40*, 329–334.

Pilquil, C., Dewald, J., Cherney, A., Gorshkova, I., Tigyi, G., English, D., Natarajan, V., and Brindley, D. N. (2006). Lipid phosphate phosphatase-1 regulates lysophosphatidate-induced fibroblast migration by controlling phospholipase D2-dependent phosphatidate generation. J. Biol. Chem. *281*, 38418–38429.

Pradere, J. P. *et al.* (2007). LPA1 receptor activation promotes renal interstitial fibrosis. J. Am. Soc. Nephrol. *18*, 3110–3118.

Ren, X. D., and Schwartz, M. A. (2000). Determination of GTP loading on rho. Methods Enzymol. *325*, 264–272.

Sano, T., Baker, D., Virag, T., Wada, A., Yatomi, Y., Kobayashi, T., Igarashi, Y., and Tigyi, G. (2002). Multiple mechanisms linked to platelet activation result in lysophosphatidic acid and sphingosine 1-phosphate generation in blood. J. Biol. Chem. *277*, 21197–21206.

Shida, D., Kitayama, J., Yamaguchi, H., Okaji, Y., Tsuno, N. H., Watanabe, T., Takuwa, Y., and Nagawa, H. (2003). Lysophosphatidic acid (LPA) enhances the metastatic potential of human colon carcinoma DLD1 cells through LPA1. Cancer Res. *63*, 1706–1711.

Sugimoto, N., Takuwa, N., Okamoto, H., Sakurada, S., and Takuwa, Y. (2003). Inhibitory and stimulatory regulation of rac and cell motility by the G12/13-rho and Gi pathways integrated downstream of a single G protein-coupled sphingosine-1-phosphate receptor isoform. Mol. Cell. Biol. *23*, 1534–1545.

Sugimoto, N., Takuwa, N., Yoshioka, K., and Takuwa, Y. (2006). Rho-dependent, rho kinase-independent inhibitory regulation of rac and cell migration by LPA1 receptor in Gi-inactivated CHO cells. Exp. Cell Res. *312*, 1899–1908.

Tanaka, M., Okudaira, S., Kishi, Y., Ohkawa, R., Iseki, S., Ota, M., Noji, S., Yatomi, Y., Aoki, J., and Arai, H. (2006). Autotaxin stabilizes blood vessels and is required for embryonic vasculature by producing lysophosphatidic acid. J. Biol. Chem. *281*, 25822–25830.

Tager, A. M. *et al.* (2008). The lysophosphatidic acid receptor LPA(1) links pulmonary fibrosis to lung injury by mediating fibroblast recruitment and vascular leak. Nat. Med. *14*, 45–54.

Umezu-Goto, M. *et al.* (2002). Autotaxin has lysophospholipase D activity leading to tumor cell growth and motility by lysophosphatidic acid production. J. Cell Biol. *158*, 227–233.

van der Bend, R. L., de Widt, J., van Corven, E. J., Moolenaar, W. H., van Blitterswijk, W. J. (1992). The biologically active phospholipid, lysophosphatidic acid, induces phosphatidylcholine breakdown in fibroblasts via activation of phospholipase D comparison with the response to endothelin. Biochem. J. *285*, 235–240.

van Leeuwen, F. N., Olivo, C., Grivell, S., Giepmans, B. N., Collard, J. G., and Moolenaar, W. H. (2003). Rac activation by lysophosphatidic acid LPA1 receptors through the guanine nucleotide exchange factor Tiam1. J. Biol. Chem. *278*, 400–406.

van Meeteren, L. A. (2006). Autotaxin, a secreted lysophospholipase D, is essential for blood vessel formation during development. Mol. Cell. Biol. *26*, 5015–5022.

van Meteren, L. A., and Moolenaar, W. H. (2007). Regulation and biological activities of the autotaxin-LPA axis. Prog. Lipid Res. *46*, 145–160.

Yanagida, K., Ishii, S., Hamano, F., Noguchi, K., and Shimizu, T. (2007). LPA4/p2y9/GPR23 mediates rho-dependent morphological changes in a rat neuronal cell line. J. Biol. Chem. *282*, 5814–5824.

Ye, X. *et al.* (2005). LPA3-mediated lysophosphatidic acid signalling in embryo implantation and spacing. Nature *435*, 104–108.